Average Power Capacity of Rotary-Field Ferrite Phase Shifters

William E. Hord, *Senior Member, IEEE*

Abstract—**The rotary-field ferrite phase shifter inherently achieves excellent phase accuracy which has led to application in many single-axis phase scanned antennas. The limitation on power capacity of this device is generally dictated by average power rather than peak power. This paper analyzes the average power capacity of the phase shifter as determined by the increase in rod temperature and the maximum thermal gradient. An equivalent circuit model for thermal analysis is developed, and its parameters are determined by r-f and temperature measurements. An alternative geometry is described which results in significantly improved average power capacity without noticeable degradation of r-f performance. An experimental phase shifter using the alternative technique was built and tested. Comparison with a conventional rotary-field phase shifter demonstrates the improvement achieved.**

Introduction

The PHASE characteristics of the rotary-field ferrite phase shifter are determined by the magnitude of the control currents applied to the drive coil of the phase shifter [1]. Since these may be set accurately, the phase shifter inherently achieves excellent phase accuracy. This, together with the relatively large peak and average power capacity of the device, has led to applications in several single-axis phase scanned antennas. The peak power capacity of the garnet material used in these devices may be modified over a rather large range of values by either substituting for some of the iron ions [2] or by controlling the grain size of the material [3]. Because of this, power limitations on antenna design are generally imposed by the average power capacity of the phase control device.

The average power capacity of garnet devices is governed by the rate of heat removal from the material. The heat is generated by dielectric and magnetic losses in the garnet with the latter generally being the major contributor. In addition there are conductor losses in the metal waveguide walls which house the garnet material. If the temperature of the material becomes excessive, or if the thermal gradients become too large, the device will cease to operate as designed and failure—sometimes catastrophic—will occur.

A cross-section of the rotary-field phase shifter is shown in Fig. 1. A circular garnet rod and steel drive yoke are contained within an aluminum housing. For high power units, a finned surface is either attached to the housing or machined directly into the housing to provide increased cooling area. An equivalent circuit, useful for examining the physical limitations on average power capacity, is given in Fig. 2. Here, P_d represents the r-f power dissipated in the phase shifter, θ_r is the internal thermal resistance of the ferrite rod, θ_{sc} is the thermal resistance from rod surface to the case, and θ_{ca} is the thermal resistance from case to ambient. The quantities T_r, T_s, T_c and T_a are the temperatures of the rod, the rod surface, the case and the ambient respectively. The measurement of rod surface temperature, case temperature and ambient temperature can be accomplished easily and accurately.

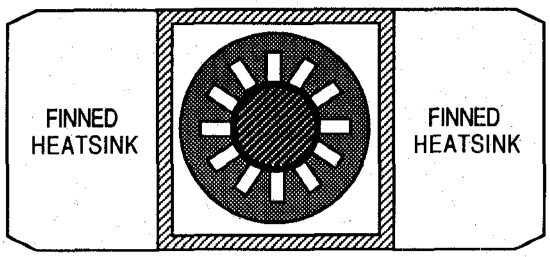

Fig. 1. Cross-section of rotary-field phase shifter.

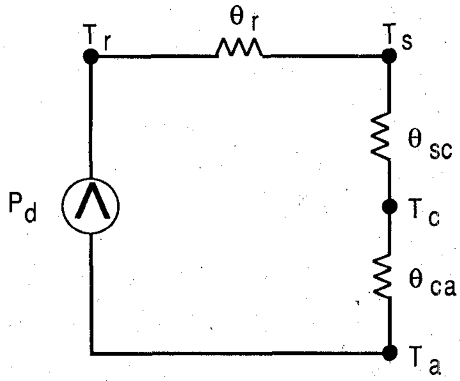

Fig. 2. Equivalent circuit for thermal analysis of phase shifter.

Temperature Distribution in the Garnet Rod

The steady-state flow of heat is governed by the equation:

$$\nabla^2 T = -\frac{A_o}{K_f} \tag{1}$$

Manuscript received March 31, 1992; revised July 28, 1992.
The author is with the Microwave Applications Group, 3030 Industrial Parkway, Santa Monica, CA 93455.
IEEE Log Number 9203711.

0018-9480/92$03.00

where T is the temperature, A_o is the volumetric rate of heat generation and K_f is the thermal conductivity of the garnet. The length of the garnet rod will be assumed to be much greater than the rod diameter so that axial variations in temperature may be ignored. Also, the rate of heat generation has been shown [4] to be nearly uniform so that A_o in (1) may be written

$$A_o = \frac{P_d}{\pi a^2 L} \tag{2}$$

where P_d is the total r-f power dissipated as heat in the rod, **a** is the radius of rod and L is the rod length. Taking the surface of the rod ($r = a$) as the reference temperature ($T = o$) and solving (1) subject to the stated assumptions yields

$$T(r) = \frac{P_d}{4\pi a^2 L K_f}(a^2 - r^2). \tag{3}$$

The thermal resistance of the garnet rod may be determined by dividing the temperature gradient from the center of the rod to the rod surface by the power dissipated in the volume. This gives

$$\theta_r = \frac{1}{4\pi L K}\ {}^\circ C/\text{Watt}. \tag{4}$$

Periodically loading a garnet rod with low-loss material of high dielectric constant, in order to achieve operation at L-band frequencies, has been successfully demonstrated [5]. The same technique may be used to increase the average power capacity of the phase shifter by inserting dielectric spacers between garnet disks as shown in Fig. 3. This geometry increases the average power capacity by allowing heat to flow from the garnet to the dielectric and then to the yoke, as well as the radial flow of heat directly from garnet to yoke. The internal thermal resistance of the rod is decreased substantially, and the thermal resistance of the rod to yoke is also decreased since the same amount of heat (approximately) is flowing over a longer length. The dielectric used for spacing the garnet disks must exhibit very low r-f loss and should have high thermal conductivity. Alumina and magnesia are two materials with low r-f loss and thermal conductivities greater than garnet by a factor of 3 for alumina and 4 for magnesia.

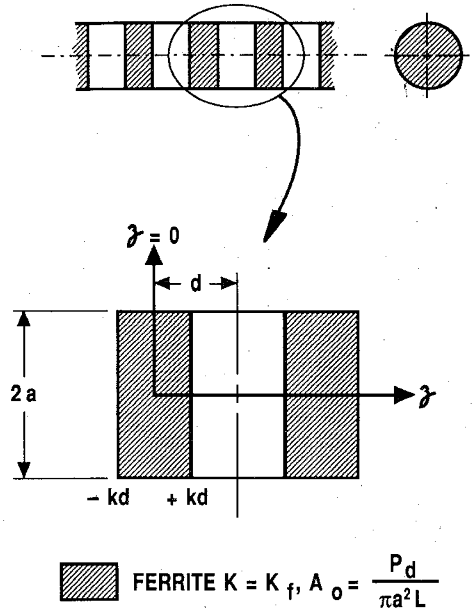

Fig. 3. Garnet rod with periodic dielectric loading.

An analytic expression for the temperature may be obtained by solving Eq. (1) subject to the boundary conditions

$$\left.\frac{\partial T_f}{\partial z}\right|_{z=0} = \left.\frac{\partial T_d}{\partial z}\right|_{z=d}$$

$$T_f|_{z=kd} = T_d|_{z=kd}$$

$$K_f \left.\frac{\partial T_f}{\partial z}\right|_{z=kd} = K_d \left.\frac{\partial T_d}{\partial z}\right|_{z=d}$$

in which z is the longitudinal distance from the center of the ferrite, d is the longitudinal distance from the center of the ferrite to the center of the dielectric spacer and k is the ratio of the length of ferrite to length of dielectric spacer. Assuming solutions of the form

$$t(r, z) = \sum_{n=1}^{\infty} \phi(z)\, J_o(\alpha_n r)$$

where $J_o(\alpha_n a) = 0$, substituting into (1) and satisfying the boundary conditions result in the following expressions for temperature in the ferrite and dielectric regions

$$T_f = \frac{2P_d}{\pi L K_f} \sum_{n=1}^{\infty} \frac{J_o(\alpha_n r)}{(\alpha_n a)^3 J_1(\alpha_n a)} \left\{ \frac{\tanh\,[(\alpha_n(1-k)_d]\,[\cosh(\alpha_n z) - \cosh(\alpha_n kd)] + \frac{Kf}{Kd}\sinh(\alpha_n kd)}{\tanh\,[\alpha_n(1-k)d]\cosh(\alpha_n kd) + \frac{Kf}{Kd}\sinh(\alpha_n kd)} \right\} \tag{5}$$

$$T_d = \frac{2P_d}{\pi L K_d} \sum_{n=1}^{\infty} \frac{J_o(\alpha_n r)}{(\alpha_n a)^3 J_1(\alpha_n a)} \left\{ \frac{\tanh\,[\alpha_n kd]\cosh\,[\alpha_n(z-d)]}{\sinh\,[\alpha_n(1-k)d] + \frac{Kf}{Kd}\tanh(\alpha_n kd)\cosh\,[\alpha_n(1-k)d]} \right\} \tag{6}$$

These expressions are plotted in Fig. 4 for the temperature at the center of the rod ($r = o$) as a function of position along the rod. In all cases, the temperature has been normalized by dividing (5) or (6) by $P_d/4\pi LK_f$ which is the temperature at the center of the rod in the absence of dielectric loading. The thermal resistance of the rod will be taken to be the average value of the temperature of the rod divided by the power dissipated. Referring to the curve for $k = 0.5$ of Fig. 4, and averaging the temperature over the road length, results in an average normalized temperature of 0.275 corresponding to a decrease in thermal resistance by a factor of 3.64 from the continuous rod.

It is relatively easy to calculate the amount of heat flowing from the ferrite to the dielectric and then to the external sink. The heat flow across a boundary may be determined from

$$Q = -\int_s K \frac{\partial T}{\partial n} dS$$

Evaluating this at $z = kd$ and normalizing by the total power dissipated gives

$$\frac{Q\text{end}}{Q\text{total}} = 4\left(\frac{a}{kd}\right) \sum_{n=1}^{\infty} \frac{1}{(\alpha_n a)^3} \cdot \left\{ \frac{\tanh[\alpha_n(1-k)d] \tanh(\alpha_n kd)}{\tanh[\alpha_n(1-k)d] + \frac{Kf}{Kd}\tanh(\alpha_n kd)} \right\} \tag{7}$$

Catastrophic failure of the garnet rod can occur if thermal gradients within the rod result in mechanical stresses severe enough to fracture the rod. For the continuous rod, the maximum thermal gradient occurs at the surface of the rod and has value

$$\left|\frac{dT}{dr}\right|_{\max} = \frac{P_d}{2\pi a L K_f} \ ^\circ\text{C/meter} \tag{8}$$

The periodic loaded rod has a longitudinal gradient as well as a radial component. The radial component has a maximum value

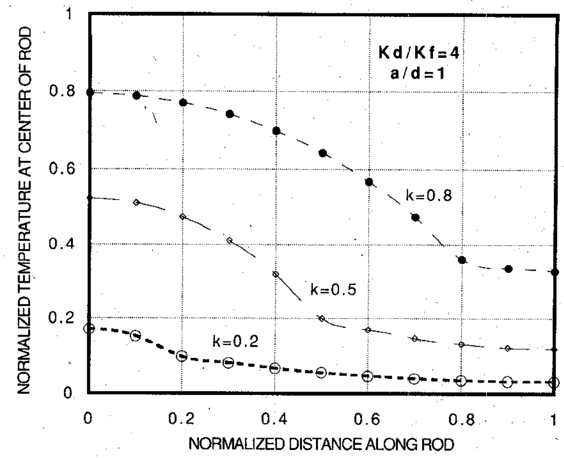

Fig. 4. Temperature distribution along composite rod.

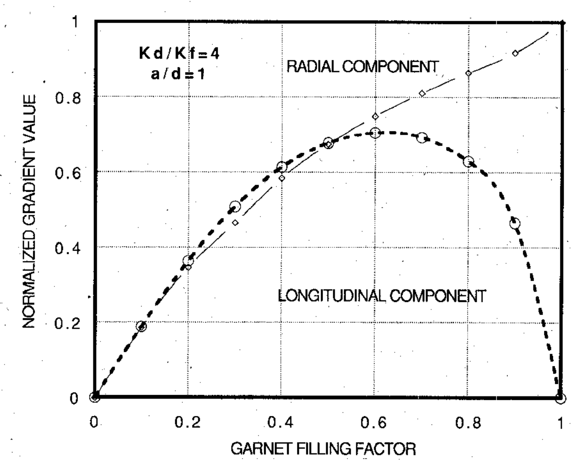

Fig. 5. Thermal gradients as a function of garnet filling factor.

These gradients are plotted in Fig. 5 as a function of the ferrite filling factor. Each gradient is normalized by dividing by (10) which is the gradient in the absence of dielectric loading. It is obvious from these curves that thermal gradients have not been increased by the dielectric loading, but neither have they been significantly decreased except for quite small ferrite filling factor which is not a particularly useful geometry. It is interesting that

$$\left|\frac{\partial T}{\partial r}\right|_{\max} = \frac{2P_d}{a\pi LK_f} \sum_{n=1}^{\infty} \frac{1}{(\alpha_n a)^2} \frac{\tanh[\alpha_n(1-k)d][\cosh(\alpha_n kd) - 1] + \frac{Kf}{Kd}\sinh(\alpha_n kd)}{\tanh[\alpha_n(1-k)d]\cosh(\alpha_n kd) + \frac{Kf}{Kd}\sinh(\alpha_n kd)} \tag{9}$$

which occurs at the center of the ferrite section ($z = o$) and the rod surface ($r = a$). The longitudinal component of the gradient has a maximum value occurring at the center of the rod ($r = o$) and at the ferrite-dielectric boundary ($z = kd$) with value

$$\left|\frac{\partial T}{\partial z}\right|_{\max} = \frac{2P_d}{a\pi LK_f} \sum_{n=1}^{\infty} \frac{1}{(\alpha_n a)^2 J_1(\alpha_n a)} \frac{\tanh[\alpha_n(1-k)d]\tanh(\alpha_n kd)}{\tanh[\alpha_n(1-k)d]\cosh(\alpha_n kd) + \frac{Kf}{Kd}\sinh(\alpha_n kd)} \tag{10}$$

the longitudinal gradient which is introduced by the dielectric loading never exceeds the radial gradient for all filling factors and is not a factor in limiting power handling capacity.

Experimental Phase Shifter

A composite rod was formed by bonding garnet disks to magnesia disks and then grinding the assembly in a centerless grinder. The rod was placed in a thin-walled aluminum tube, and matching transformers were added at both ends. The drive yoke was placed over the aluminum tube, and this assembly was placed in a finned aluminum housing. A temperature sensor was placed on the aluminum tube in order to monitor the surface temperature of the garnet rod. Another temperature sensor was located on the phase shifter housing at the base of the cooling fins. The ambient temperature was monitored by standard means.

Low power r-f measurements were taken in order to verify the insertion loss, phase accuracy and insertion phase variation with temperature of the experimental phase shifter. The low power insertion loss was approximately 0.5 dB over the operating band which compares favorably with the conventional design. The phase characteristics of the device were essentially identical with the conventional design with the phase shifter exhibiting roughly 5 degree phase offset between clockwise and counterclockwise rotation of bias field which is a measure of the hysteresis associated with the phase shifter. This number which is typical of rotary-field phase shifters is generally removed in practice by the application of a "backup" angle which guarantees that the final angle is always approached from the same direction.

Figure 6 shows the variation of the insertion phase of the device as a function of ambient temperature. The slope of this curve (0.526 degrees r-f per degree Celsius) is typical for this class of phase shifters. However, the intent of measuring the insertion phase vs. ambient temperature is to use the insertion phase as a measure of the average temperature of the rod. Since the saturation magnetization of the garnet varies with temperature, the insertion phase of the unit will vary with temperature and will provide a fairly accurate measure of the average rod temperature.

The phase shifter was subjected to high power testing using a pulsed high power source operating at a duty cycle of 0.0333. The input power was increased gradually to a maximum of 3000 Watts average which was the limit of the source. Cooling air was blown over the surface of the fins. The insertion loss of the device, the rod surface temperature and the case temperature were continually monitored as the power level was increased. Throughout the test the phase shifter showed no indications of excessive heating. The insertion phase was measured by removing the high power signal from the unit and quickly measuring the phase by switching a low power network analyzer into the waveguide test system.

Figure 7 gives the increase in the rod surface temperature and case temperature as a function of the average input power. For a 0.5 dB insertion loss, the dissipated power is 11 percent of the input power. Using these figures, the thermal resistance θ_{sc} may be calculated to be 61°C/KW and the case-to-ambient thermal resistance to be 39°C/KW. The insertion phase increased 24.5 electrical degrees as the average power was increased from 0 to 3000 W. This corresponds to a rod temperature increase of 46.6°C from ambient. The increase in rod sur-

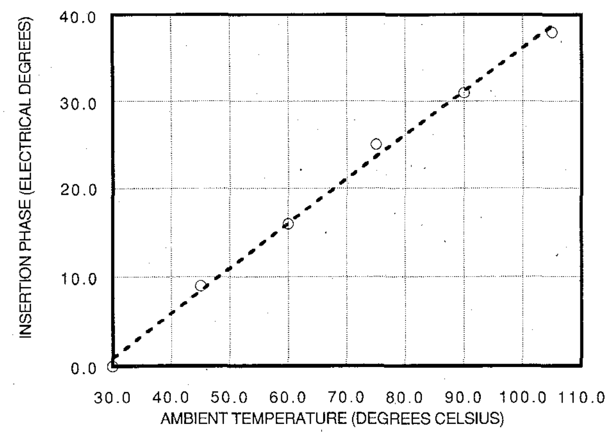

Fig. 6. Variation of insertion phase with ambient temperature.

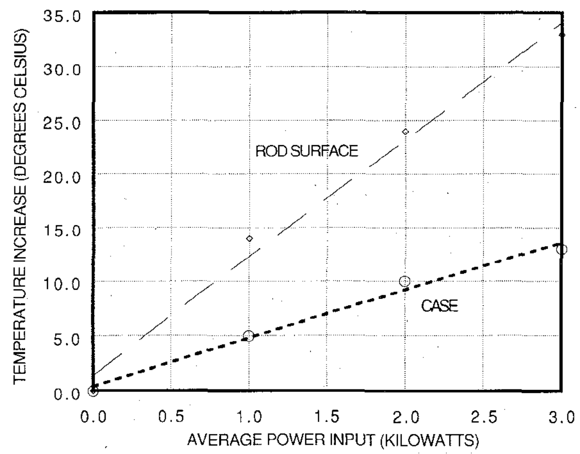

Fig. 7. Case and rod surface temperature increase as a function of input power.

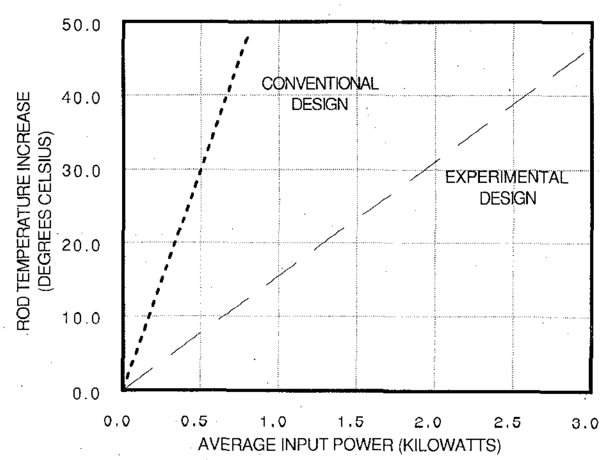

Fig. 8. Comparison of experimental design with conventional phase shifter design.

TABLE I
THERMAL RESISTANCE COMPARISON

	Thermal Resistances in °C/KW			
	θ_r (calc.)	θ_r (meas.)	θ_{sc} (meas.)	θ_{ca} (meas.)
Conventional	250	222	234	136
Experimental	69	40	36	39

face temperature was 33°C, so that the thermal resistance θ_r is calculated to be 40°C/KW.

It is of interest to compare the values of the thermal resistances obtained for the experimental phase shifter with thermal resistances of the conventional rotary-field phase shifter. The conventional model tested exhibited an insertion phase change of 27 electrical degrees when operated at rated average power of 800 W. This corresponds to a rod temperature 48°C above the ambient. The rod temperature increase as a function of the average input power is shown in Fig. 8 for both phase shifters. The thermal resistances are compared in the Table I.

CONCLUSIONS

A technique has been described to increase the average power capacity of the rotary-field ferrite phase shifter by alternating layers of dielectric with the garnet. This allows the r-f energy dissipated as heat within the garnet material to be extracted from the ends of the garnet as well as the curved surface of the rod. The boundary value problem governing the behavior of the composite structure was solved, and the temperature distribution in the garnet and dielectric was presented. Expressions for the thermal gradients were developed, and the maximum value of thermal gradient was plotted as a function of the garnet filling factor.

An air-cooled experimental phase shifter was fabricated and tested at both low and high r-f power levels. The low power testing indicated that the phase shifter performance was substantially equivalent to the conventional rotary-field design. The high power testing indicated the experimental unit had about five times the average power capacity of the conventional design. A simple equivalent circuit for the flow of heat in the device was presented and values of the resistances for the experimental phase shifter were compared with those of the conventional rotary-field device.

ACKNOWLEDGMENT

The author is pleased to acknowledge the support of Microwave Applications Group for the work presented here. In particular, discussions with Dr. Charles Boyd were extremely helpful. The experimental phase shifter was assembled and tested by Charles Oness and James Tracy.

REFERENCES

[1] C. R. Boyd, Jr., "An accurate analog ferrite phase shifter," in *1971 IEEE Int. Microwave Symp. Dig.*, June 1971, pp. 104–105.

[2] J. J. Green and F. Sandy, "A catalog of low power loss parameters and high power thresholds for partially magnetized ferrites," *IEEE Trans. Microwave Theory Tech.*, vol. MTT-22, no. 6, pp. 645–651, June 1974.

[3] C. E. Patton, "Effect of grain size on the microwave properties of polycrystalline yttrium iron garnet," *J. Applied Physics*, vol. 41, p. 1637, 1970.

[4] C. R. Boyd, Jr., L. R. Whicker, and R. W. Jansen, "Study of insertion phase variation in a class of ferrite phasers," *IEEE Trans. Microwave Theory Tech.*, vol. MTT-18, no. 12, pp. 1084–1089, Dec. 1970.

[5] C. R. Boyd, Jr., and C. M. Oness, "Ferrite rotary-field phase shifters with reduced cross-section," in *1990 IEEE Int. Microwave Symposium Dig.*, May 1990, pp. 1003–1006.

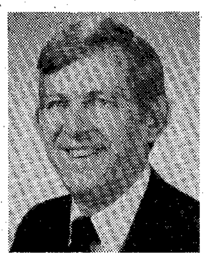

William E. Hord (S'57–M'60–SM'78) was born in Leola, South Dakota, in 1938. He received the BSEE from the Missouri School of Mines and Metallurgy, Rolla in 1959, the MSEE in 1963, and Ph.D. in 1966 from the University of Missouri at Rolla.

His teaching experience is as an Instructor of Electrical Engineering form 1960 to 1966 at the University of Missouri at Rolla, a part-time Assistant Professor at the Graduate Engineering Center, University of Missouri at Rolla during 1967–1968 and Professor of Engineering at Southern Illinois University. At SIU he was Chairman of the Department of Engineering from 1974 to 1981 and Acting Dean of the School of Engineering from 1983 to 1984. He worked at the Sperry Gyroscope Co. from 1959 to 1960 on the development of high-power klystrons. From 1966 to 1968 he worked at the Emerson Electric Co. on the development of airborne phased-array antenna, in particular, the RARF antenna. In 1984 he joined the Microwave Applications Group where he is presently Vice President of Engineering. His activities are concerned with the development and application of ferrite phase shifters to phased-array radar.

Dr. Hord is a member of Eta Kappa Nu, Phi Kappa Phi, Sigma Xi and Tau Beta Pi. He was named Outstanding Electrical Engineering Teacher in St. Louis Section IEEE in 1984. He currently serves as Co-Chairman of the MTT Technical Committee on Microwave Ferrites.